MINISTRY OF SCIENCE AND HIGHER EDUCATION OF THE RUSSIAN FEDERATION
FEDERAL STATE AUTONOMOUS EDUCATIONAL INSTITUTION HIGHER EDUCATION

"National Research Nuclear University "MEPhI"

Institute of Nuclear Physics and Technology

Small Thesis

"Quark-Gluon Blob in interaction of Ultra High Energy Cosmic Rays"

Student Abroo Uruj

Group M21-192

Lecturer M. Yu. Khlopov

Moscow 2022

CONTENTS

LIST OF FIGURES

1 INTRODUCTION

High energy particles such as protons, photons and heavy nuclei, from extragalactic, galactic or solar origin are called cosmic rays. These primary cosmic rays, on entering the earth's atmosphere interact with nuclei in the atmosphere and produce what is called an air shower of secondary particles.

The global view of total energy spectrum of cosmic rays is as shown in Figure 1.

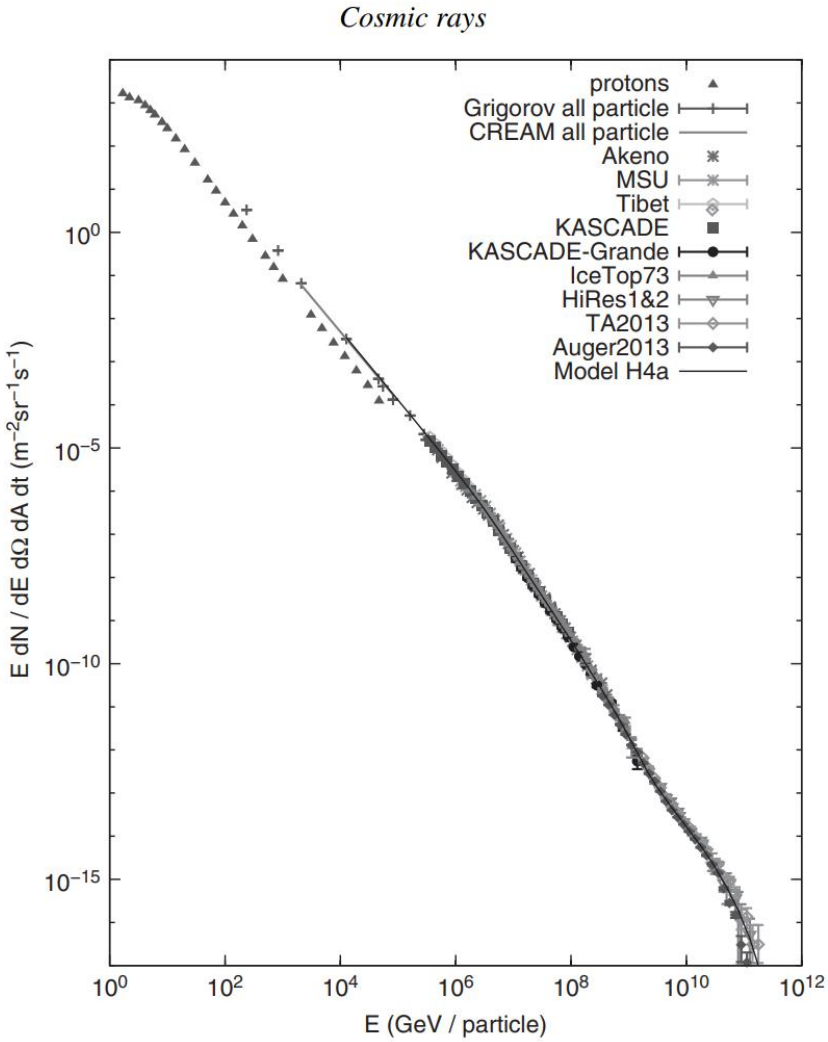

Figure 1: Energy spectrum of cosmic rays [1]

The point on the spectrum at about 3.10^{15}eV where the slope changes is called the knee and further, at about 3.10^{18}eV, where the slope changes again is called the ankle. [1]

Observations of various phenomena relating to cosmic rays can be interpreted in either cosmological approach, where all changes are ascribed to changes in energy and/or composition of primary cosmic rays, or nuclear-physical approach, i.e. based on the interaction model. Usually, the first approach is considered, where it is assumed that the energy of air showers is equal to that of the primary cosmic rays producing them. This perspective results in difficulties in explanation of many observations [2]. As is listed in the next section.

1.1 UNEXPLAINED EVENTS

At very high energies i.e. greater than 10^{15} eV, some observed events are inexplicable within the current theoretical purview [3][4]. The most puzzling characteristics of ultrahigh energy cosmic rays as observed in different experiments are listed below:

• In hadron experiments:

- Families- Sets of separated cascades [5]
- Halos around cascade families- Diffused dark shadows around some cascade families
- Alignment of cascades, despite the probability of such random occurrence is negligible
- Highly penetrating cascades
- Centauros i.e. families of multiple hardon cascades without an accompanying electromagnetic cascade [5]
- long-flying component that has high penetration before producing a cascade [6]
- Anti-Centauros i.e. electromagnetic cascade without hardon cascade [7]

• In muon experiments:

- Excess of very high energy (VHE~ 100 TeV) single (MSU) and multiple (LVD) muons[8]
- Observation of VHE muons, even if the probability to detect such muons is very small. [9]

• In Extensive Air Shower (EAS) investigations: [10]

- Young and old showers, large p_t, etc;
- EAS spectrum change in atmosphere, usually interpreted as a change of primary energy spectrum;
- Nμ(Ne) and Xmax(Ne) dependences change behaviour, explained as a change of the composition towards heavier elements.[11]

1.2 REQUIREMENT OF NEW INTERACTION MODEL

Therefore, the second approach i.e. nuclear-physical, can be considered instead. The main assumption of this alternate approach is that the energy of the EAS is not equal to the energy of the primary particles. Also, the new model of interaction that can explain all of the above listed observations would require to have the following characteristics:[3]

1. Threshold behaviour; since unusual events appear above several PeV only.
2. Large cross section; in order to change the slope of the EAS spectrum.
3. Large yield of leptons; to explain the excess of VHE muons and missing energy.
4. Large orbital (or rotational) momentum; to explain alignment of decay products and its large lifetime.
5. Very fast development of EAS; to increase Nμ/Ne ratio and decrease Xmax elongation rate.

2 QUARK GLUON HYPOTHESIS

All the above requirements are met if blobs of quark gluon matter with large orbital momentum are produced in non-central nucleus-nucleus collision that occur when high energy primary comic ray particles collide with the nuclei in the atmosphere at energies greater than several PeV [2][3]. It is important to note here, quark gluon matter implies partons in liquid state that allows collective quark and gluon interaction as opposed to plasma, which implies gas where collective interactions are not possible.

Quark gluon matter (QGM) production automatically meets the first requirement of threshold behaviour since production of QGM requires some high energy (temperature). Because of many quarks and gluons interacting in place of single pair of quark-quark integration, geometrical cross section will be changed from $\sigma = \pi\lambda^2$ (for quark- quark interactions) to $\sigma = \pi(\lambda + \mathrm{R})^2$ or $\sigma \sim (R_1 + R_2)^2$ where R, R1, R2 are sizes of interacting quark-gluon matter blobs. If R reaches even the size of nucleons, it will be sufficient to reach the necessary value of cross section.

Globally polarised QGM with large angular orbital momentum *L* is produced in non-central ion-ion collisions. *L* increases with increase in collision energy in center of mass system $L \sim \sqrt{s}$[12].

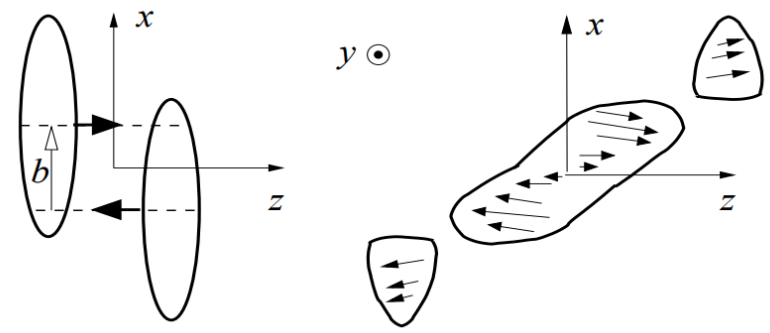

Figure 2: Non-central heavy-ion collisions with impact parameter ~b. The global angular momentum of the produced matter is along − ˆ y, opposite to the reaction plane. [12]

The centrifugal barrier of the QGM increases with L and thus with the collision energy $\sqrt{s}$. The blob here can be considered to be in resonance state with increased lifetime, with a large centrifugal barrier. This centrifugal force has a value in centre of mas system of $V(L) = L^2/mR^2$. Thus, the centrifugal barrier will be lower for heavier quarks and the probability of its decay will be larger. This results in the suppression of light quark production, and thus provides enough time for appearance of heavy t quarks (or other heavy particles) in the very hot QGM. [13]

Figure 3: Centrifugal barrier for particles with different masses: left – light mass, right – heavy mass.[3]

This top quark (or any other heavy particle with mass $\gtrsim 100$ GeV/c^2, taking into account fly out energy) will decays into W or Z boson.

$$eg: t(\bar{t}) \rightarrow W^+(W^-) + b(\bar{b}) \quad [14]$$

Here W- boson and
b – quark

3 QGM MODEL EXPLAINING THE OBSERVED ANOMALIES

The bosons thus produced will decay into hadrons (probability ≈ 70%, on average, and ≈30% pions) which explains appearance of excess of muon bundle, due to multiplicity of the secondary particles produced [3]. Correspondingly EAS development varies which can explain young and old showers, large values of transverse momentum, etc.

Alternatively, decay of the W bosons into lepton pairs (ev_e, μv_μ, τv_τ with probability ≈10% per each pair) can account for the missing energy as these neutrinos are not detected and the muon energy is not measured either. The energy of these muons and neutrinos will be very large (more than 100 TeV) and thus the measured energy of EAS can sufficiently differ from the primary particle energy, causing a knee in measured spectrum.

Penetrating cascades can be explained too. VHE muons can produce similar events. The flux of VHE muons from known sources with necessary energies (~ 1 PeV) is very small. However, the flux at these energies increase by at least two orders due to muons from decays of heavy particles (through W, Z-bosons).

Centauros and other such unusual events' probability is increased, as in weak interactions, there is non-conservation of isospin and only charged particle production will be possible.

3.1 CALCULATIONS AND COMPARISON WITH EXPERIMENTAL DATA

Collision energy changes because of simultaneous interaction of many quarks:

$$\sqrt{s} = \sqrt{2m_N E_1} \rightarrow \sqrt{2m_C E_1}$$

where m_N = nucleon mass and
m_C is compound mass of many interacting quarks.
For calculations, one can consider $m_C = nm_N$, (n = 1÷ A).

Production of $t\bar{t}$ -quark pair must decrease $\sqrt{s}$ at least by the value of $2m_t$, and in a general case by some value $\varepsilon_t > 2m_t \approx 350GeV$ which will depend on primary particle energy and its mass. The residual part of the energy in the center of mass system ($\sqrt{s} - \varepsilon_t$) will be converted into the energy of usual processes of EAS development. In the first approximation, for simplification, part of the energy taken away by top-quarks and re-injected into EAS development, is

neglected. So, results of standard measurements and standard procedure of evaluation of EAS energy will give value E_2

$$E_2 = \frac{(\sqrt{2m_C E_1} - \varepsilon_t)^2}{m_C}$$

which is less than the energy of the primary particle E_1,and we will obtain the steepening of the observed spectrum

Transition from E_1 to E_2 gives a bump near the threshold as shown in Figure 4 [2]

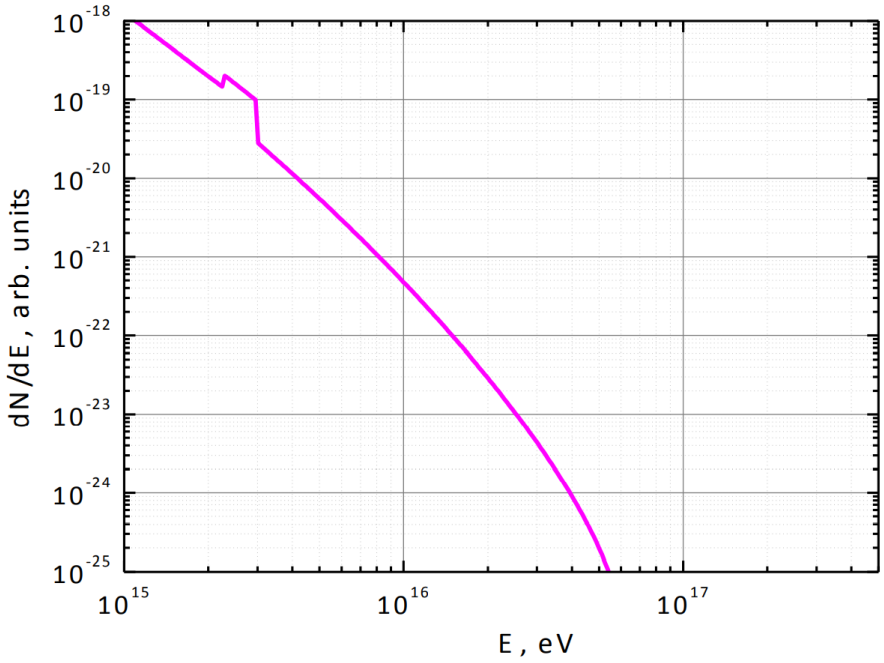

Figure 4: Formation of measured cosmic ray energy spectrum in frame of nuclear-physical approach.[2]

As high density is required for the production of QGM, the threshold energy for production of new state of matter will be lesser for heavier nuclei compared to that for lighter nuclei. Thus, it is assumed that at first QGM is produced in iron nuclei (or any other heavier nuclei) interactions. Following this increasingly lighter nuclei produce the QGM. This is shown if the Figure 5.

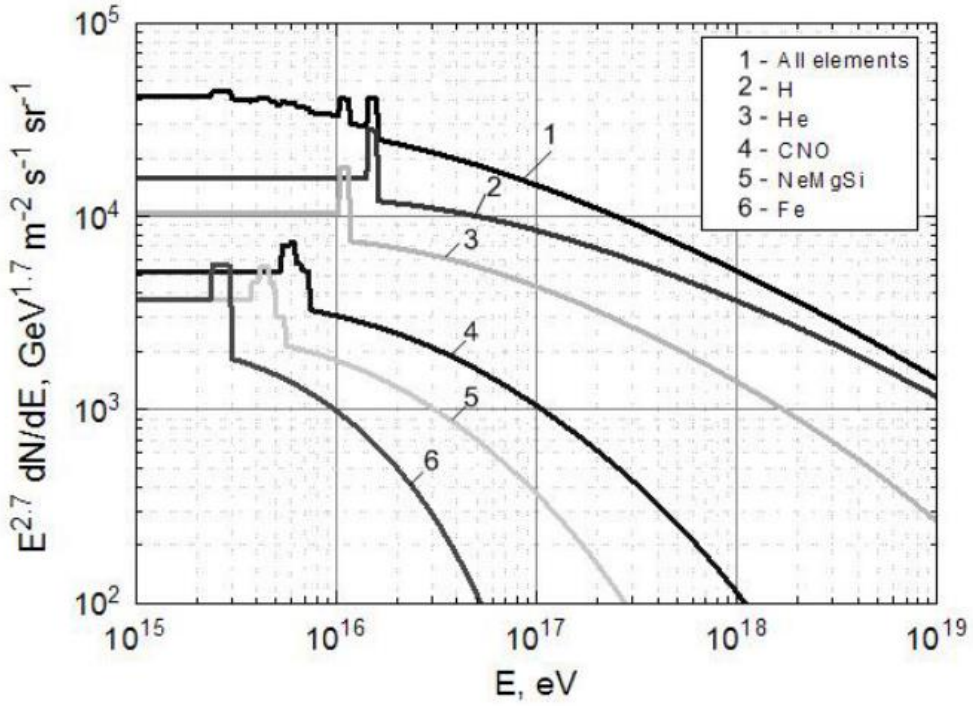

Figure 5: Changes of various nuclei spectra in the frame of the considered model. [2]

For calculations primary spectra values for various nuclei were taken from [15]

The results of calculations assuming 15% straggling of measured energies and comparison with experimental data on all particle spectrum are given in Figure 6. Also on average the part of interacting nucleons does not exceed one quarter of the total number of nucleons of both nuclei. [16]

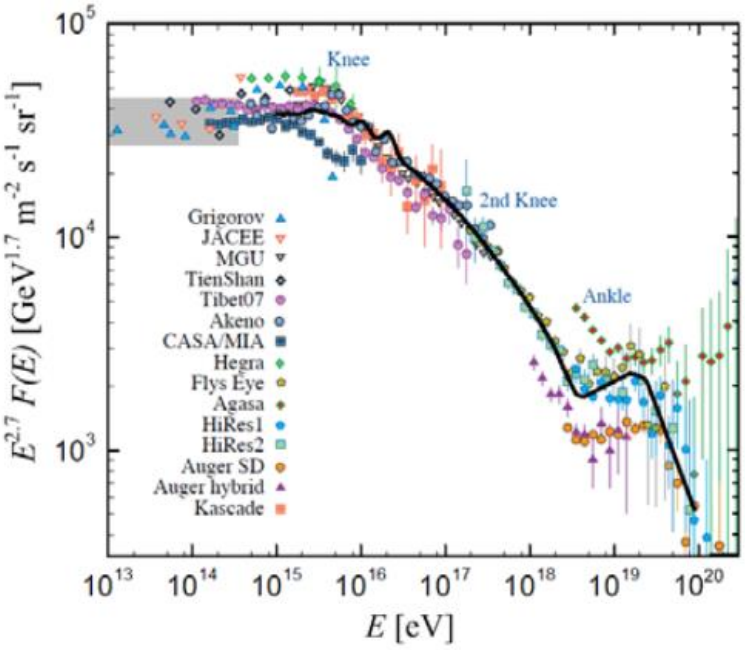

Figure 6: Calculated and experimental data.[2]

4 QGM HYPOTHESIS IN EXPERIMENTS

4.1 SUBSTANTIATING POSTULATE

At the Relativistic Heavy Ion collider (RHIC), during Au-Au collisions at $\sqrt{s} = 200$ GeV, the total angular orbital momentum L of the overlapping system as a function of impact parameter b, obtained is shown in the Figure 7 [13], [17]. Also shown in the plot, is the curve in dashed line for a hard sphere (which will not gain a large angular momentum upon non central impact). Comparing the two curves it becomes clear that the postulate about increased Woods - Saxon potential with increase in momentum for heavier particles is true.

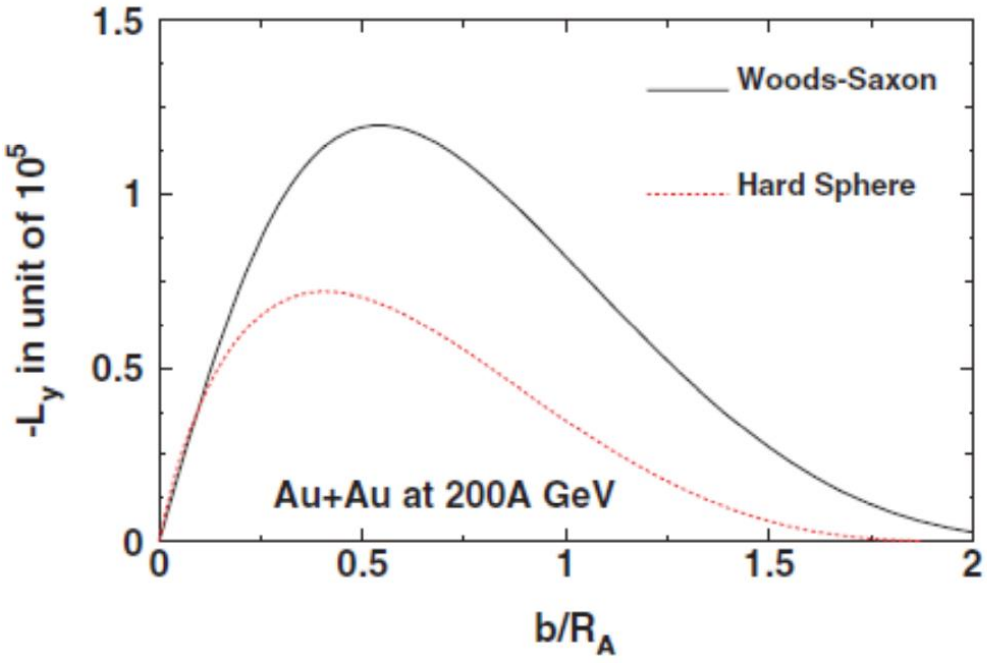

Figure 7: Total orbital angular momentum of the overlapping system in Au+Au collisions at the RHIC energy as a function of the impact parameter b.[13]

4.2 IN EAS INVESTIGATIONS

Upon simulation of EAS cascade while including the production of top-pair in its development, excess of muons with energy ~100 TeV appears, if the production of blobs of QGM starts at energies of several PeV[14]. Thus, potentially resolving muon puzzles.

Practically, this hypothesis can be directly proven by either accurately measuring the energy spectrum of atmospheric muons above energies of 100TeV or by

showing that excess of VHE muons appear in interactions of primary particles with energy above the knee and are absent below the knee. [3].

The dependence of the excess of muon bundles on the energy of primary cosmic rays, for six existing interaction models, that were registered by all the different installations that registered multiple muons generated by primary cosmic rays of ultrahigh energies is as shown in Figure 8 [18]. The largest contribution in the energy range from 10^{14} to 10^{20} eV was made by three installations: NEVOD, Pierre Auger, and IceCube. The experiment at MEPhI covers the largest energy range, in the lower energy region it is proved by the IceCube data and by Pierre Auger in the ultrahigh energy region [19].

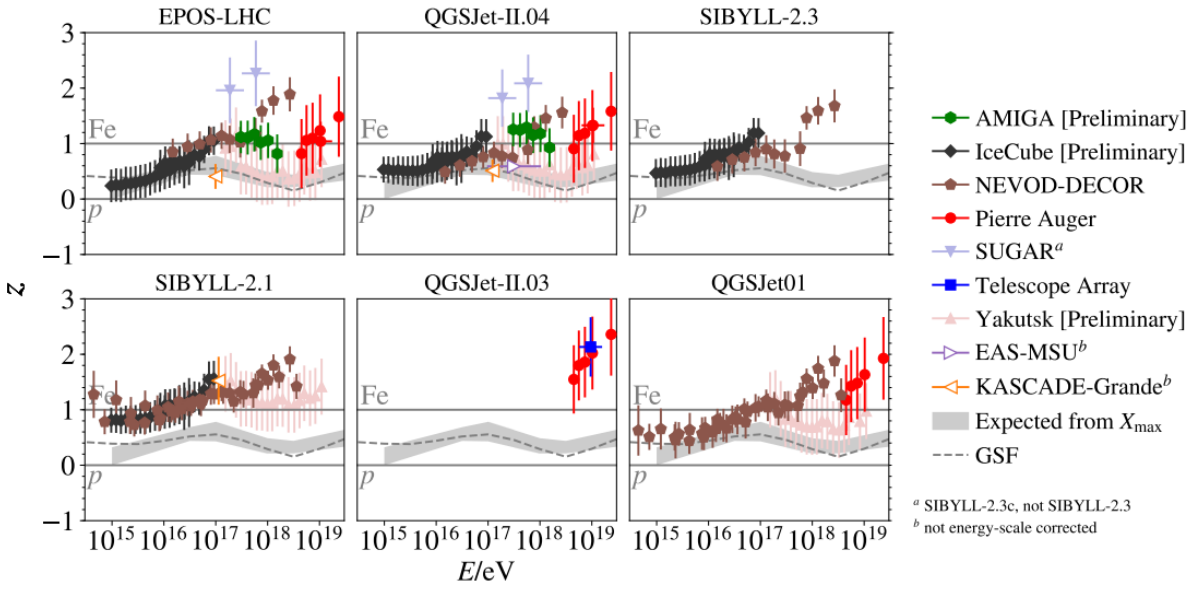

Figure 8: Dependence of the magnitude of the excess of bundles of muons on the energy of primary cosmic rays for six existing models of interactions.[18]

According to the data of measurements of bundles of muons at the NEVOD-DECOR complex [20]–[22] in the range of zenith angles of 65° -75°, corresponding to the energies of primary particles above 10^{17} eV, an increase in the average energy of muons in bundles was found in comparison with the results of calculations using modern post-LHC models of hadronic interactions, which may indicate a change in the interaction model [23].

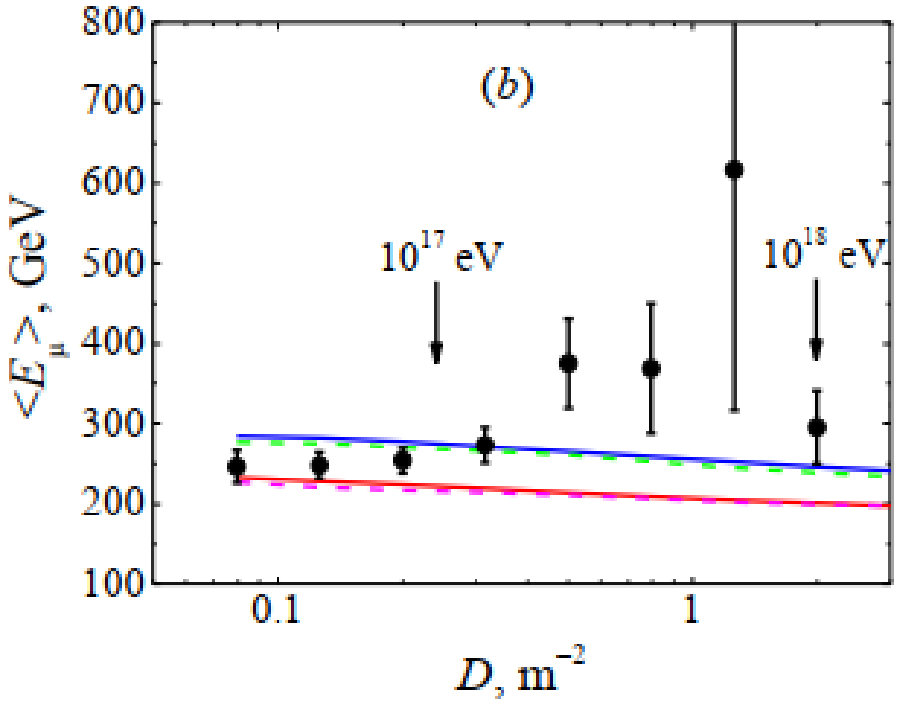

Figure 9: Dependence of the average energy of muons in the bundles on the local muon density for the interval of zenith angles θ = 65⁰ - 75⁰The dots are experimental data and the curves are the expected dependences for EAS muon bundles formed by primary protons (red line) and iron nuclei (blue line). The arrows show the characteristic energies of cosmic ray primary particles. [23].

The inclusion of a new coordinate-track detector TREK[24][25] in the NEVOD experimental complex will allow to expand the range of investigated energies to the interval from 10^{14} to 10^{19}eV[26], which will cover the entire region in which an excess of cosmic ray muons is observed. To improve the accuracy of muon bundle energy deposit measurement, the extension and optimization of Cherenkov water detector structure will be done [27]. An increase in the accuracy in determining the multiplicity of bundles and their energy deposit will make it possible to understand the nature of the muon puzzle and give an answer about the inclusion of the QGM hypothesis in the interaction of primary cosmic rays of ultrahigh energies.

4.3 In Colliders

The observation of transversally-unbalanced two-jet events with energy ~100 GeV in lead-lead collisions at $\sqrt{S_{NN}} = 2.76TeV$ with the ATLAS detector at LHC can be explained by this hypothesis [28], [29]. In the t-quark decay, the energy in its rest frame is distributed as $T_b \approx 65$ GeV and $T_W \approx 25$ GeV. With its motion taken into account, the total energy can amount to ~100 GeV. The b-quark jet and the W-boson decay to ~20 pions will form an event pattern observed in the ATLAS experiment, as shown in Figure 10.

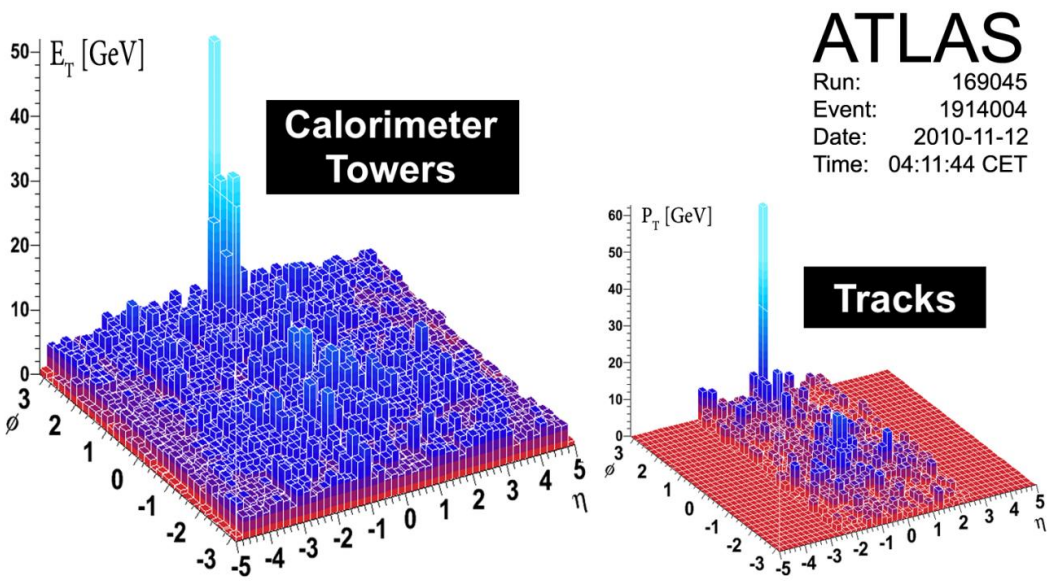

Figure 10: An event with two jets strongly unbalanced in transverse momentum[29]

Also, with increasing collision energy, the multiplicity of secondary particles was found to increase faster in Pb–Pb collisions than in p–p collisions [30] , but for the former the collision energy was estimated as that of the nucleon– nucleon interaction,$\sqrt{S_{NN}}$. In nucleus–nucleus interactions, if the actual target is heavier than the nucleon, the c.m.s. energy has been underestimated and the experimental points should be shifted to the right. Since the multiplicity of secondary particles cannot be less in nucleus–nucleus than in p–p collisions, this will allow one to estimate the number of nucleons that form the target in nucleus–nucleus collisions (see Figure 11). The shift of experimental points is determined by the quantity $n_N$estimated as

$$\sqrt{n_N} = \frac{\sqrt{S_{AA}}}{\sqrt{S_{NN}}} < \frac{40 - 45\ TeV}{3TeV} \approx 14$$

We can conclude that in Pb–Pb collisions, up to a half of the total number of constituent nucleons of the two nuclei can form a QGM blob.

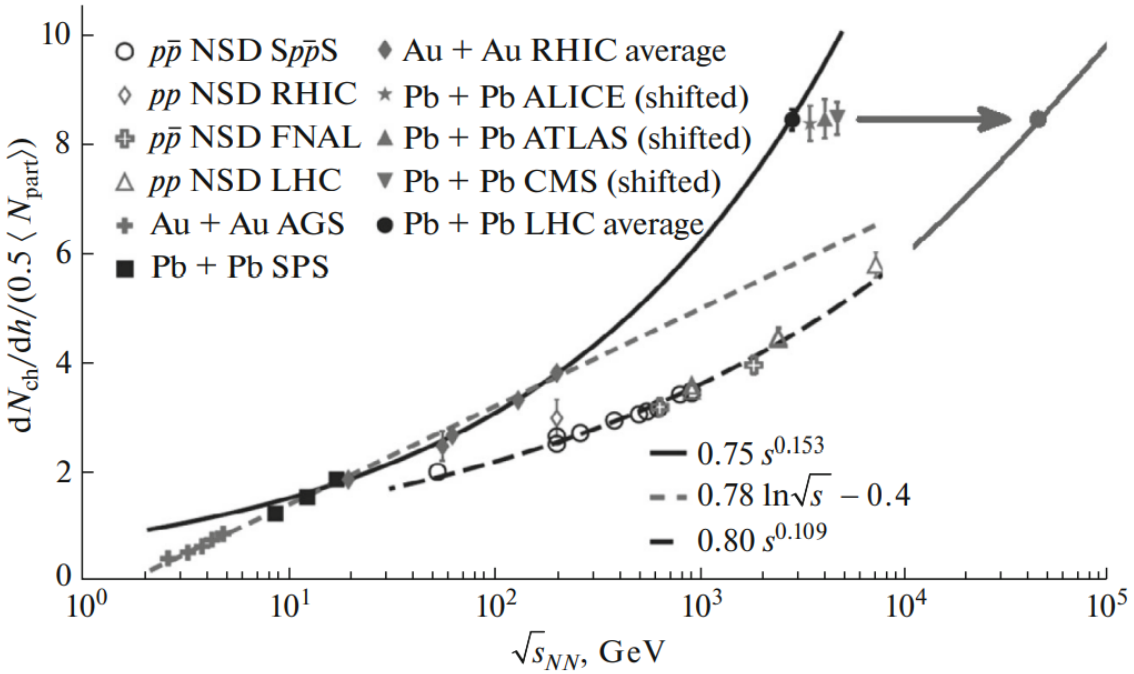

Figure 11: Multiplicities of charged particles formed in nucleus–nucleus and proton–proton collisions as a function of collision[30]

4.4 Relation between Cosmic ray and collider experiments

In the case of nitrogen–nitrogen collisions the energy 10^{15} eV in cosmic rays corresponds to 2.65 TeV in collider beams[31]. But there exists an essential difference between cosmic ray and collider experiments, which is illustrated in Figure 12. In collider experiment QGB has practically zero velocity and decays isotropically at least for equal nuclei, though some elliptic effects were observed [32]. Other nucleons of colliding nuclei keep primary directions of movement and go away without registration in detector systems; so in collider experiments only energy transferred in QGB is measured. In CR we measure not only the QGB energy but also the energy which is determined by the number of nucleons which fly towards the Earth after the first interaction. The total number of nucleons is defined as $A_f = A_1 + \Delta A_2$, which depends on the type of the primary nuclei and can change from A_1 to $A_1 + A_2$ (for nitrogen and more heavy nuclei).[31]

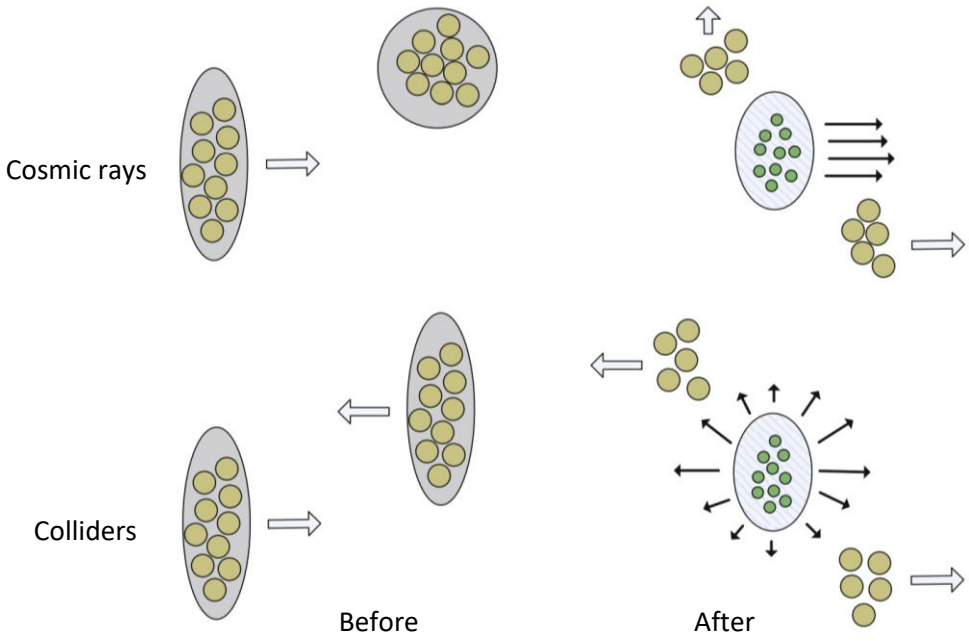

Figure 12: Difference between collider and cosmic ray experiments.[31]

5 CONCLUSION

Anomalies observed in ultrahigh energy cosmic ray spectrum are discussed.

Hypothesis of production of Quark Gluon Blobs when ultrahigh energy cosmic ray particles collide with nuclei in the atmosphere and the consequences following it are detailed.

Experimental results that support the postulates of the hypotheses, that can be explained by the QGM hypothesis and which can further validate this hypothesis in the future are discussed, along with elucidating the difference in interpretation of data between the collider and cosmic ray experiments as per this hypothesis.

6 REFERENCES

[1] T. K. Gaisser, R. Engel, and E. Resconi, *Cosmic {Rays} and {Particle} {Physics}*, 2nd ed. Cambridge: Cambridge University Press, 2016. doi: 10.1017/CBO9781139192194.

[2] A. A. Petrukhin, 'Cosmic rays above the knee: experimental results and their interpretation', p. 4.

[3] A. A. Petrukhin, 'Manifestations of quark-gluon plasma in cosmic ray experiments', *Nuclear Physics B - Proceedings Supplements*, vol. 175–176, pp. 125–128, Jan. 2008, doi: 10.1016/j.nuclphysbps.2007.10.020.

[4] V. M. Maximenko, V. S. Puchkov, S. E. Pyatovsky, S. A. Slavatinsky, and R. A. Mukhamedshin, 'Some interesting phenomena observed in cosmic-ray experiments by means of x-ray emulsion technique at super accelerator energies', p. 16.

[5] E. Gladysz-Dziadus, 'Are {Centauros} exotic signals of the {QGP}?', *arXiv:hep-ph/0111163*, Jan. 2012.

[6] A. O. Herrera *et al.*, 'EDITORA DA DIVERSIDADE ESTADUAL DE CAMPINAS {Reitor}: {J} ». -• {Aristodemo} {Pinotti}', p. 260.

[7] V. I. Yakovleva, 'Anti-{Centaur0} type events at energies 5-500 {TeV} detected by the {Tien}-{Shan} {EAS} complex', p. 1.

[8] A. A. Petrukhin, 'muon excess.pdf'. Conference Proceedings Vol. 85, 'Frontier Objects in Astrophysics and Particle Physics' P.527, p. 12, 2003.

[9] E. Iarocci and S. Ragazzi, 'Cosmic-Muon Results from the NUS] ~ X Experiment .', 1986.

[10] S. B. Shaulov *et al.*, 'Investigation of EAS cores', *EPJ Web of Conferences*, vol. 145, no. November, p. 17001, 2017, doi: 10.1051/epjconf/201714517001.

[11] A. Aab *et al.*, 'Depth of maximum of air-shower profiles at the Pierre Auger Observatory. I. Measurements at energies above $10^{17.8}$eV', *Physical Review D*, vol. 90, no. 12, p. 122005, 2014, doi: 10.1103/PhysRevD.90.122005.

[12] Z. T. Liang and X. N. Wang, 'Globally polarized quark-gluon plasma in noncentral A + A collisions', *Physical Review Letters*, vol. 94, no. 10, pp. 1–5, 2005, doi: 10.1103/PhysRevLett.94.102301.

[13] J. H. Gao, S. W. Chen, W. T. Deng, Z. T. Liang, Q. Wang, and X. N. Wang, 'Global quark polarization in noncentral A+A collisions', *Physical Review C - Nuclear Physics*, vol. 77, no. 4, pp. 1–13, 2008, doi: 10.1103/PhysRevC.77.044902.

[14] A. A. Petrukhin, 'Muon puzzle in cosmic ray experiments and its possible solution', *Nuclear Instruments and Methods in Physics Research Section A: Accelerators, Spectrometers, Detectors and Associated Equipment*, vol. 742, pp. 228–231, Apr. 2014, doi: 10.1016/j.nima.2013.12.011.

[15] P. D. Group, 'University of Zurich', *Journal of Clinical Epidemiology*, vol. 58, no. 5, p. I, 2005, doi: 10.1016/s0895-4356(05)00103-4.

[16] A. A. Petrukhin, E. S. Sozinov, and V. V. Shutenko, 'Possible approach to the analysis of nucleus-nucleus interactions at very high energies', *J. Phys.: Conf. Ser.*, vol. 1181, p. 012090, Feb. 2019, doi: 10.1088/1742-6596/1181/1/012090.

[17] Z.-T. Liang and X.-N. Wang, 'Globally Polarized Quark-gluon Plasma in Non-central A+A Collisions', *Phys. Rev. Lett.*, vol. 94, no. 10, p. 102301, Mar. 2005, doi: 10.1103/PhysRevLett.94.102301.

[18] E. A. Zadeba and A. A. Petrukhin, 'A MegaScience class experimental complex at the University', *J. Phys.: Conf. Ser.*, vol. 2210, no. 1, p. 012014, Mar. 2022, doi: 10.1088/1742-6596/2210/1/012014.

[19] H. P. Dembinski *et al.*, 'Report on Tests and Measurements of Hadronic Interaction Properties with Air Showers', *EPJ Web Conf.*, vol. 210, p. 02004, 2019, doi: 10.1051/epjconf/201921002004.

[20] A. G. Bogdanov *et al.*, 'Investigation of very high energy cosmic rays by means of inclined muon bundles', *Astroparticle Physics*, vol. 98, pp. 13–20, Mar. 2018, doi: 10.1016/j.astropartphys.2018.01.003.
[21] A. G. Bogdanov *et al.*, 'Intensity of muon bundles according to the NEVOD-DECOR cosmic ray experiment', *J. Phys.: Conf. Ser.*, vol. 1690, no. 1, p. 012007, Dec. 2020, doi: 10.1088/1742-6596/1690/1/012007.
[22] E. A. Yurina *et al.*, 'Investigation of the Energy Loss of Muon Bundles in the Cherenkov Water Calorimeter', *Phys. Atom. Nuclei*, vol. 82, no. 6, pp. 680–684, Nov. 2019, doi: 10.1134/S1063778819660505.
[23] E. A. Yurina *et al.*, 'Status of the NEVOD–DECOR Experiment on the Study of Muon Bundles Energy Deposit', *Bull. Russ. Acad. Sci. Phys.*, vol. 85, no. 4, pp. 455–457, Apr. 2021, doi: 10.3103/S1062873821040390.
[24] E. A. Zadeba *et al.*, 'The coordinate-tracking detector based on the drift chambers for ultrahigh-energy cosmic ray investigations', *J. Inst.*, vol. 9, no. 08, pp. C08018–C08018, Aug. 2014, doi: 10.1088/1748-0221/9/08/C08018.
[25] E. A. Zadeba *et al.*, 'The detector on the basis of drift chambers for inclined muon bundle investigations', *J. Inst.*, vol. 12, no. 07, pp. C07005–C07005, Jul. 2017, doi: 10.1088/1748-0221/12/07/C07005.
[26] E. A. Zadeba *et al.*, 'Investigation of muon bundles generated by UHECR by means of the new coordinate-tracking detector', *J. Phys.: Conf. Ser.*, vol. 1390, no. 1, p. 012132, Nov. 2019, doi: 10.1088/1742-6596/1390/1/012132.
[27] S. S. Khokhlov *et al.*, 'Studying the Characteristics of Optical Modules in the Volume of the NEVOD Cherenkov Water Detector', *Bull. Russ. Acad. Sci. Phys.*, vol. 85, no. 4, pp. 452–454, Apr. 2021, doi: 10.3103/S106287382104016X.
[28] A. A. Petrukhin and A. G. Bogdanov, 'Heavy particles at the LHC and in cosmic rays', *Phys. Part. Nuclei*, vol. 48, no. 5, pp. 793–795, Sep. 2017, doi: 10.1134/S1063779617050343.
[29] The ATLAS Collaboration, 'Observation of a Centrality-Dependent Dijet Asymmetry in Lead-Lead Collisions at sqrt(S(NN))= 2.76 TeV with the ATLAS Detector at the LHC', *Phys. Rev. Lett.*, vol. 105, no. 25, p. 252303, Dec. 2010, doi: 10.1103/PhysRevLett.105.252303.
[30] K. Aamodt *et al.*, 'Charged-Particle Multiplicity Density at Midrapidity in Central Pb-Pb Collisions at s N N = 2.76 TeV', *Phys. Rev. Lett.*, vol. 105, no. 25, p. 252301, Dec. 2010, doi: 10.1103/PhysRevLett.105.252301.
[31] E. S. Sozinov, A. G. Bogdanov, A. A. Petrukhin, and V. V. Shutenko, 'Simple Geometrical Model of Nucleus—Nucleus Interactions at Very High Energies', *Phys. Atom. Nuclei*, vol. 82, no. 6, pp. 929–933, Nov. 2019, doi: 10.1134/S1063778819660463.
[32] K. Aamodt *et al.*, 'Elliptic Flow of Charged Particles in Pb-Pb Collisions at s N N = 2.76 TeV', *Phys. Rev. Lett.*, vol. 105, no. 25, p. 252302, Dec. 2010, doi: 10.1103/PhysRevLett.105.252302.